Direct Synthesis of Nanowires with Anatase and TiO_2-B Structures at near Ambient Conditions

Walid A. Daoud*,† and G. K. H. Pang‡

Nanotechnology Center, ITC and Department of Applied Physics, The Hong Kong Polytechnic University, Hung Hom, Hong Kong

Received: July 14, 2006; In Final Form: October 3, 2006

In this study, we present a new approach toward titanium oxide nanowires. In this approach, the growth formation of the wires sets in at a temperature as low as 40 °C under ambient pressure. Moreover, we provide evidence that nanowires with distinctive TiO_2-anatase and TiO_2-B structures can be directly produced without further thermal treatment using controlled reaction conditions.

Introduction

Oxide nanotubular materials have recently been receiving growing interest.[1] Among these materials, titanium oxide nanotubes in particular have received tremendous interest due to their potential use in a countless number of applications, such as in photocatalysis, solar energy conversion, gas sensing, electrochromic displays, and rechargeable lithium batteries as insertion electrodes.[2]

The first synthesis of TiO_2 nanotubes with relatively large diameters (70−100 nm) was achieved using a polymer mold, on which titanium dioxide was deposited electrochemically.[3] Much smaller tubes (∼10 nm in diameter) were surprisingly synthesized by a simple soft chemistry approach.[4] In this approach, anatase, rutile, or their mixtures are hydrothermally treated with a concentrated NaOH aqueous solution in an autoclave and subsequently washed with a dilute HCl solution. These tubes were originally characterized as composed of the anatase structure.[5] Detailed investigation of the structure of these tubes by Du et al. suggested that the nanotubes are composed of layered hydrogen trititanate $H_2Ti_3O_7$.[5] Sun and Li confirmed that these nanotubes are titanate, not TiO_2, and that the as-synthesized tubes can be described as $Na_xH_{2-x}Ti_3O_7{\cdot}yH_2O$ ($x = 0.75$).[6] Some later studies argued in favor of an anatase structure of the tubes,[7] while other groups suggested that they are composed of tetratitanate ($H_2Ti_4O_9{\cdot}H_2O$)[8] or lepidocrocite titanate ($H_xTi_{2-x/}\square_{x/4}O_4$, where $x = 0.7$ and $\square$ = vacancy).[9] It has also been suggested that NaOH acts as a catalyst in this hydrothermal treatment and that a high concentration of Na^+ cations and strong basic conditions are essential in the synthesis of the nanotubes.[10]

Authors supporting the titanate structure propose that the NaOH treatment leads to the total recrystallization of the starting TiO_2 material into lamellar sodium titanate, followed by the peeling-off of individual titanate sheets from the crystallites because of the hydrogen deficiency of the topmost layer. This mechanism has recently been put in question by Kukovecz et al., who presented evidence against the rollup formation model.[11] They subjected synthetic $Na_2Ti_3O_7$ crystals to the typical alkaline hydrothermal treatment used in the formation of nanotubes (130 °C, 10 M NaOH, 72 h) and showed that, instead of nanotube formation, the trititanate sheets were only cut into blocks of stripes 20 nm wide and over 300 nm long. According to these authors, the nanotubes' formation proceeds via oriented crystal growth of seeds of nanoloops that are formed by local concentration fluctuations on the crystallite surface during the alkali treatment.[11]

It is clear that the structure and formation mechanisms of the products of the alkaline hydrothermal treatment are still controversial and frequently debated in the literature. Likewise, the occasionally studied KOH treatment reaction has also witnessed a certain degree of controversy, as demonstrated by contemporary literature. Nakahira et al. claimed that the use of either NaOH or KOH in the hydrothermal treatment (110−150 °C, 20−168 h) of anatase or rutile titania leads to hydrated tetratitanate nanotubes ($H_2Ti_4O_9{\cdot}H_2O$) with morphologies varied with the structure of the starting material, hydrothermal reaction time, and temperature.[8] Nevertheless, the tubular morphology of the KOH reaction products cannot be verified, as they were not shown in their report. On the other hand, Peng et al. showed that the KOH hydrothermal reaction (130 °C, 72 h) leads to the formation of nanowires of hexatitanate composition ($K_2Ti_6O_{13}$).[12] Yuan and Su also reported that the KOH hydrothermal reaction (130−240 °C, 24−48 h) produces neither tubular nor ribbonlike but wirelike products that were indexed as octatitanate ($K_2Ti_8O_{17}$).[13]

In this contribution, we demonstrate that TiO_2 nanowires can be directly produced by the KOH reaction under ambient pressure and temperature and that the phase of the formed nanowires can be controlled as TiO_2-anatase and TiO_2-B by the reaction temperature.

Experimental Details

In the formation of nanotubes, single-phase anatase with an average grain diameter of about 4−6 nm was used as starting material.[14] The synthesis of the nanotubes was carried out by adding the as-prepared anatase powder to a 10 M KOH solution. Parallel reactions were run at different temperatures, namely, 40, 60, 80, and 110 °C in an oil bath for 72 h under reflux and ambient pressure. The products were filtered by centrifugation at 3000 rpm, washed twice with water, 0.05 M HCl solution, and finally acetone. This was followed by drying at 80 °C for 16 h.

* Corresponding author. E-mail address: tcdaoud@polyu.edu.hk.
† Nanotechnology Center, ITC.
‡ Department of Applied Physics.

10.1021/jp064453n CCC: $33.50
Published on Web 12/01/2006

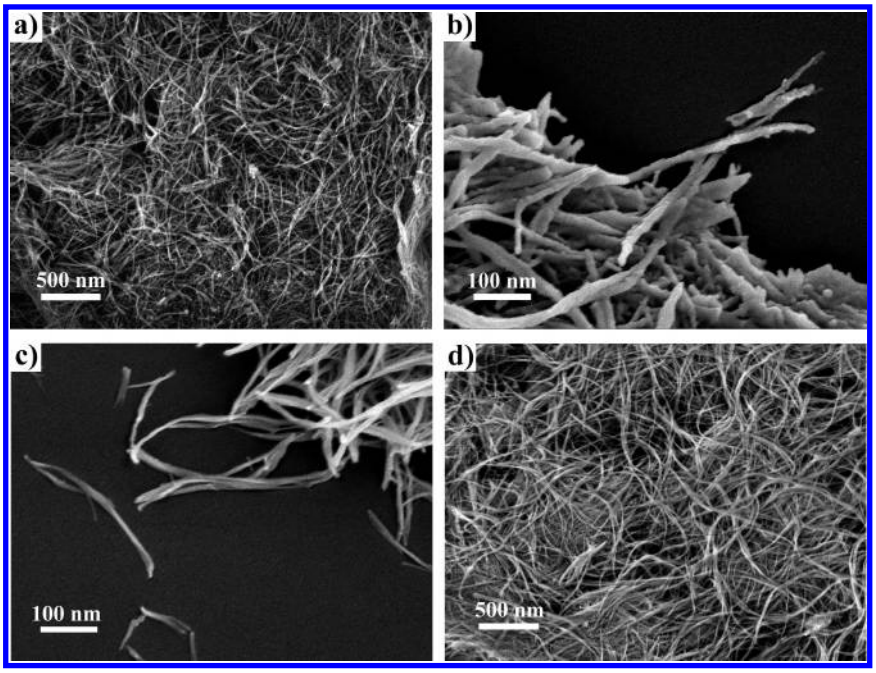

Figure 1. (a) Low-magnification FESEM image of the nanowires formed at 40 °C. High-magnification FESEM images of the nanowires showing individual nanotubes formed at (b) 60 and (c) 80 °C. (d) Low-magnification image of the nanowires formed at 110 °C.

Powder X-ray diffraction was performed with Cu Kα radiation on a Bruker D8 Advance X-ray diffractometer operating at 40 kV and 30 mA. Raman spectra were acquired by Renishaw RM3000 Micro-Raman system with 20 mW excitation at 519 nm of Ar laser and detection limit at 200 cm^{-1} due to the Notch filter cutoff.

The morphology of the collected powders was investigated using a field emission scanning electron microscope JEOL JSM-6335F operated at 3 kV and a scanning electron microscope Leica Stereoscan 440 operated at 20 kV and equipped with Oxford energy-dispersive X-ray system.

High resolution transmission electron microscopy was performed on a JEOL JEM-2011 and field emission JEOL JEM-2010F operated at 200 kV and equipped with EDX facilities. To prepare the HRTEM specimens, the powder samples were first dispersed ultrasonically in acetone. One drop of the suspension was placed on a carbon film supported on a copper grid and allowed to dry in air before the specimens were transferred into the microscope.

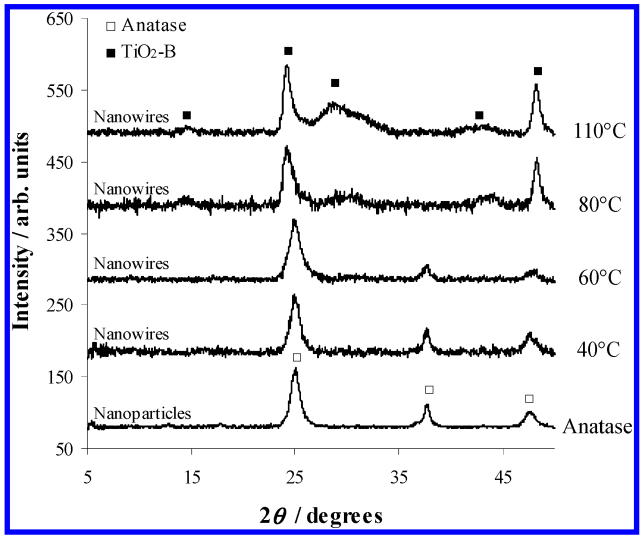

Figure 2. XRD patterns of the reaction products prepared at different temperatures. Powder diffraction pattern for TiO_2 anatase starting material is shown for reference.

Results and Discussion

Our interest lies in the examination of the KOH reaction under ambient pressure using our recently synthesized single-phase anatase nanocrystallites with grains of 4−6 nm diameter that were prepared by a near room temperature method.[14] We were motivated by a recent report that showed the smaller the size of the starting material, the milder the reaction parameters in the hydrothermal treatment of TiO_2.[9] The reaction was carried at 110 °C under ambient pressure instead of the light overpressures typically applied in the hydrothermal synthesis using autoclaves. In the first instance, the structure of the fibrous products shown in Figure 1 was originally thought to be titanate nanotubes. However, careful XRD investigation (Figure 2) of the product revealed the absence of the most intense peak of the titanate structure at $2\theta \approx 10°$ suggesting that the formed product were composed of TiO_2 and not titanate.

It has recently been shown that at higher temperatures (170−200 °C) the NaOH hydrothermal treatment yields nanorods[6b] and nanoribbons,[15] suggesting that temperature is crucial in controlling the final morphology of the products. In light of this, we decided to investigate the effect of reaction temperature using a fixed KOH concentration (10 M) under ambient pressure.

When the reaction temperature was reduced to 80 °C, fibrous products were obtained. These structures, which show identical XRD spectra as shown in Figure 2, were identified as TiO_2-B (a detailed discussion will be presented later on). This TiO_2-B phase was further confirmed by Raman spectroscopy.[2g] Figure S1 of the Supporting Information shows a typical Raman spectrum of the reaction products formed at temperatures above 80 °C. However, at a reaction temperature of 60 °C, fibrous structures were formed but with rather different structure than that observed at 80 and 110 °C and retaining the same phase of the original starting materials. Surprisingly, at 40 °C nanofibers with identical structure as those produced at 60 °C were also obtained. In contrast to prior reports, these fibrous structures were formed from titania grains under much milder conditions,

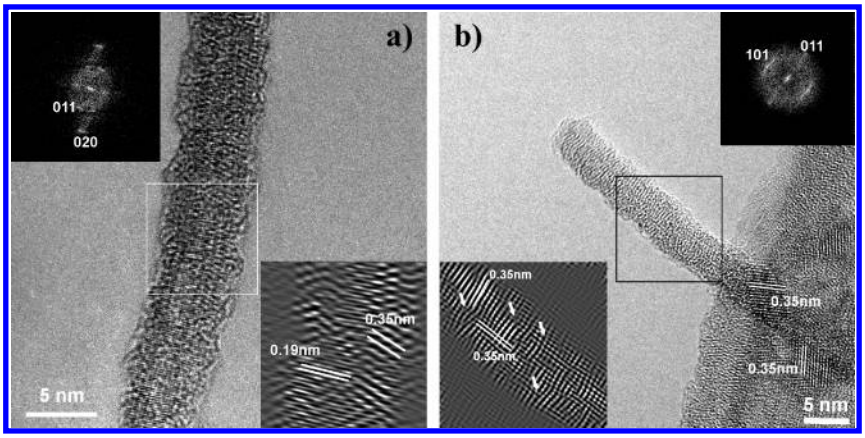

Figure 3. (a) HRTEM image of a single nanowire. The top left and bottom right insets represent the fast Fourier transformation power spectrum and the Fourier filtered image of the marked region, respectively. Both of the insets indicate that the nanowire is grown along the [020] direction. (b) HRTEM of a nanowire with few nanoparticles attached. The lattice fringes of the nanowire correspond to the [101] plane of anatase. This therefore suggests that the [101] is the other possible growth direction of the nanowire.

such as ambient pressure and temperatures, and the reaction temperature was found to be crucial in controlling the crystalline structure. The presence of a high yield of nanowires at different reaction temperatures can be demonstrated by the FESEM images shown in Figure 1.

Figure 2 shows that at temperatures $\leq$60 °C during the hydrothermal treatment with KOH, the fibrous products were anatase, as demonstrated by the retention of the anatase associated peaks at $2\theta = 25°$ (101), 37° (004), and 48° (200) of the starting material. At temperatures $\geq$80 °C, XRD analysis of the products shows the disappearance of the anatase peaks and the appearance of TiO_2-B-associated peaks. TiO_2-B can be distinguished from the anatase structure by the absence of the anatase peak at 37° (004) and from the titanate structure by its broad peak of multiple planes between 28 and 34° and by the absence of the titanate (020) peak at 10°. When the fibrous products formed at $\leq$60 °C were heated at 80 °C in 10 M KOH solution, they were also converted to TiO_2-B.

In the past, the synthesis of anatase nanowires[7,8,15] and TiO_2-B nanoribbons[15−17] could only be achieved by calcination of the titanate cylindrical products at temperatures $\geq$400 °C and it has been shown that this approach results in substantial damage or loss of their morphology. Thus, in this contribution we provide evidence that TiO_2-anatase and TiO_2-B nanowires can be directly produced by the KOH treatment without further thermal processing. Furthermore, since all previously reported nanofibers/nanowires were exclusively produced in the titanate structure using high temperatures and overpressures, this is the first direct synthesis of TiO_2 nanowires under near ambient conditions.

TiO_2 has six polymorphs, which are rutile,[18] anatase,[18] brookite,[19] TiO_2-B,[20] TiO_2 II,[21] and TiO_2 (H).[22] Among the frequently studied TiO_2 polymorphs, TiO_2-B has fairly received less attention. The structural information including the space group, density, and unit cell data were tabulated by Banfield et al.[23] All of the known TiO_2 polymorphs can be modeled as edge- and corner-linked structure with Ti cations coordinated octahedrally by oxygen anions.[24] In particular, anatase and TiO_2-B contain chains of edge-sharing octahedral in one orientation while the other polymorphs have chains in two orientations.[24] TiO_2-B and anatase are thus structurally related. TiO_2-B was first synthesized by hydrolysis of $K_2Ti_4O_9$[25] followed by filtration and heating at 500 °C and found to possess similar structure as VO_2.[26] The space group and the unit cell parameters of anatase and TiO_2-B are respectively given as follow: tetragonal *I4/amd*, $a = b = 0.378$ nm, $c = 0.951$ nm, $\beta = 90°$ [18] and monoclinic *C*2/*m*, $a = 1.216$ nm, $b = 0.374$ nm, $c = 0.651$ nm, $\beta = 107.29°$.[25] The atomic parameters were determined by the Rietveld refinement method using data from powder neutron diffraction.[27] The experimental refined atomic parameters, shown in Table S1 in the Supporting Information, were found to be in good agreement with the data calculated by Catlow et al.[28] using the energy minimization technique. The conversion of TiO_2-B to anatase, which takes place either at 550 °C and 1 atm (1.0133 bar) or room temperature and 60 kbar, was reported by Brohan et al.[29] TiO_2-B was also found as intergrowth in anatase mineral.[23] An explanation for the transformation was subsequently provided by Tournoux et al.[30] and Banfield et al.[23] The transformation from TiO_2-B to anatase occurs through crystallographic shear along the $(10\bar{3})$ plane of anatase or the $(\bar{2}01)$ plane of TiO_2-B, with the shear eliminating a similar amount of cationic and anionic vacancies.[23,29,30] The transformation follows the orientation relationship.[29] **B**/**b** and $|\mathbf{B}|/|\mathbf{b}| = 0.378$ nm/0.373 nm = 1.0134, i.e., unit cell vector **B** of anatase is parallel to the unit cell vector **b** of TiO_2-B and the angle between reciprocal vector **A*** of anatase and reciprocal vector **c*** of TiO_2-B is 6.3°.

With the advancement of nanotechnology, there has recently been a revived interest in TiO_2-B for its photocatalytic and electrochemical properties. TiO_2-B nanowires and nanotubes were synthesized[16] using layered hydrogen titanates as precursors following the original synthetic procedure.[25] It was also shown that TiO_2-B is a very good candidate for hosting Li, resulting in $Li_{0.68}TiO_2$ used in energy storage.[31]

Detailed structures of the fibrous products were investigated by high-resolution transmission electron microscopy (HRTEM) and selected area electron diffraction (SAED). To study the formation mechanism of the TiO_2 nanowires, the HRTEM investigation focused on the intermediate product of the KOH hydrothermal treatment after 24 h of reaction time. Figure S2 is a low magnification TEM of the 24-h product formed at 60 °C showing a large proportion of nanowires. The typical dimensions of the nanowires are 4−6 nm across and several micrometers long. A number of nanoparticles of 4−6 nm in diameter are found attached to the nanowires. The SAED pattern obtained from the region including both the nanoparticles and the nanowires shows the presence of single-phase anatase TiO_2. Detailed studies of these samples revealed the presence of two types of nanowires, as characterized by their difference in the direction of growth. The first type of growth is found along the [020] direction, whereas the second type grows along the [101] direction. Figure 3a shows a HRTEM image of a nanowire of

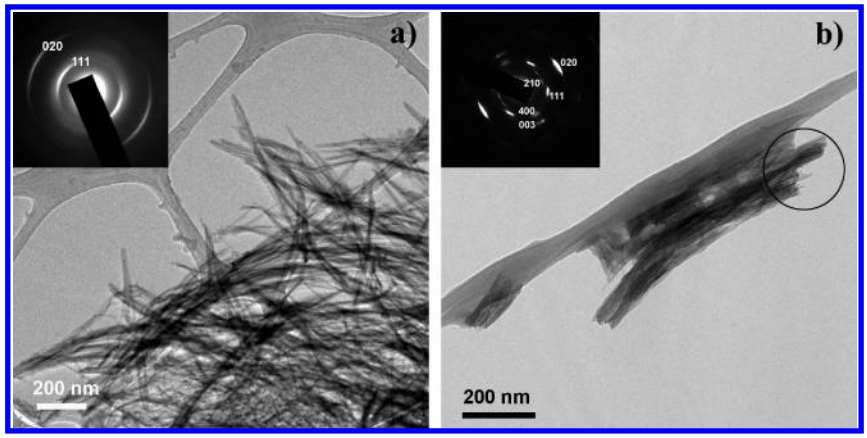

Figure 4. (a) Low-magnification TEM image of the 80 °C product together with the corresponding SAED in the inset. (b) Low-magnification TEM image showing a bundle of the nanowires formed at 110 °C. The inset is the SAED from the marked circle. The SAED of both images is indexed using the interplanar spacings of TiO_2-B.

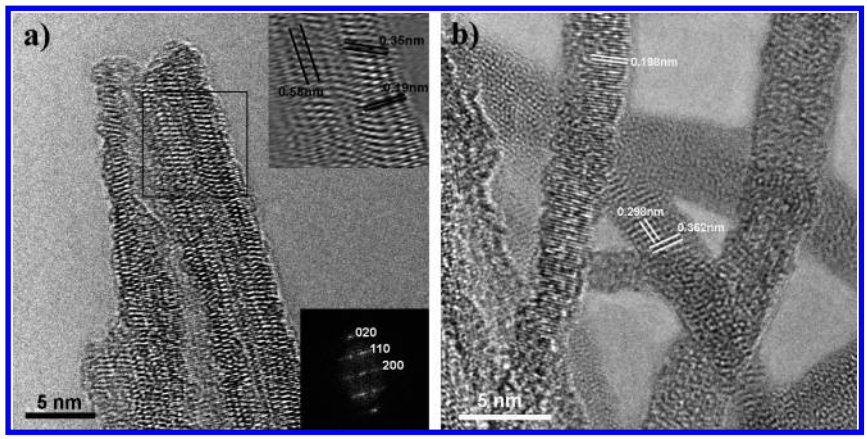

Figure 5. (a) HRTEM of TiO_2-B nanowires formed at 110 °C. The TiO_2-B (020) plane is normal to the axial direction of the nanowire, illustrating the transformation from the [020] grown anatase. (b) HRTEM of 110 °C product showing several TiO_2-B nanowires. One of the nanowires in the middle of the image shows the TiO_2-B (201) plane normal to the axial direction.

the first type with growth along the [020] plane. The inset in the top left corner of the figure is the power spectrum of the fast Fourier transformation from the marked region, and the spots are due to the (011) and (020) planes of anatase, as indicated. The corresponding filtered image in the bottom right corner shows clearly that the (020) planes, 0.19 nm wide, are normal to the growth direction. The (011) plane, as also indicated, is 0.35 nm wide and in 22° with respect to the (020) plane. These values are in good agreement with the calculated values for anatase TiO_2. Thus, it is concluded that these nanowires belong to anatase TiO_2.

Figure 3b shows a HRTEM image of the second type nanowire formed at 60 °C. The power spectrum of the marked region, inserted in the top right corner, shows the peaks corresponding to (101) and (011) planes. The corresponding filtered image is shown in the bottom left corner, and the lattice spacing of the (101) and (011) planes are marked. Because of the high density of dislocation (marked by a series of arrows in the inset), the lattice is strained, resulting in highly distorted fringes, as readily seen. However, the angle between the two sets of planes is measured to be 81°, which is very close to the calculated value of 82.1° for anatase TiO_2. The discrepancy is believed to be due to the distortion of the lattice, as seen in the figure. Figure 3b also shows several nanoparticles attached to the nanowire. The lattice spacings of 0.35 nm corresponding to the (101) planes of anatase TiO_2 are marked. Since we observed that nanoparticles were attached to the nanowire, it is here suggested the observed products represent an intermediate stage of the growth of the nanowires through joining of the nanoparticles.

In agreement with the XRD study, TEM investigation revealed that nanowires formed at temperatures $\geq$80°C are composed of TiO_2-B and not anatase. Figure 4a is a low-magnification TEM image of the 80 °C reaction product. The inset of Figure 4a shows an SAED pattern with only two strong diffracted rings and several diffused rings, which is different from typical anatase diffraction. Since we observed [020] and [101] grown anatase nanowires produced at temperatures $\leq$60 °C, it is expected that two different orientations would be observed in the TiO_2-B structure.

Figure 4b shows a low-magnification TEM image of a bundle of nanowires, and the region corresponding to the SAED pattern is marked by a circle. The SAED pattern is a typical diffraction of fibrous textures and was successfully indexed using the interplanar spacings derived from TiO_2-B, as shown in Table S2 in the Supporting Information. The indexing shows clearly that the axial direction of the nanowires in the image is normal to the (020) plane. It is here noted that the 110 °C product exhibits identical features as that formed at 80 °C.

In the discussion of the transformation from TiO_2-B to anatase, Brohan described the process in terms of a crystallographic shear along the TiO_2-B (201) plane[29] and gave the crystallographic relationship between the two phases (see Table S2). The observed axial direction of TiO_2-B, as shown previously normal to the (020) plane, is the result of the transformation from [020]-oriented anatase. We believe the transformation

mechanism follows the reverse process from TiO_2-B to anatase. Although, it contradicts the expectation, because the metastable TiO_2-B phase grows at higher temperature than the more stable anatase phase, the observed transformation is consistent with the epitaxtial relationship given by Brohan[29] for the transformation from TiO_2-B to anatase.

Figure 5 shows the HRTEM image of a TiO_2-B nanowire formed at 110 °C. The power spectrum of the marked region is shown in the bottom right inset and the corresponding filtered image is in the top right inset. The main peaks in the power spectrum are indexed as TiO_2-B (200), (110), and (020) planes. The filtered image in the inset shows the corresponding lattice fringes with the measured spacings marked on the top. Note that the axial direction of the nanowire is normal to the TiO_2-B (020) plane and it is believed to be transformed from the [020] grown anatase.

A second type of TiO_2-B nanowire with a different direction of growth, in analogy to the observed [101] grown anatase nanowire, was also observed. Figure 5b shows the HRTEM image from the product of 110 °C reaction. The marked 0.362 nm wide fringes correspond to the TiO_2-B (201) planes and are normal to the axial direction of the nanowire. Thus, the nanowire is transformed from [101] grown anatase, since the anatase (101) plane transforms to TiO_2-B (201) planes according to the above discussions.

It is clear that unlike the NaOH treatment where high temperatures $\geq$150 °C and overpressures are usually applied to produce nanowires, the KOH reaction can proceed at much lower temperatures without autoclaving. It is noteworthy to mention that no other forms of byproducts such as sheets or plates could be observed and that at any given time of the reaction only fibers with/without grains could be found, suggesting a stacking-up mechanism of the TiO_2 grains to produce a more thermodynamically stable wirelike structure, even at a temperature as low as 40 °C.

In conclusions, it has been demonstrated that ambient pressure treatment of TiO_2 with KOH leads to the formation of titanium oxide nanowires. Furthermore, the phase of these nanowires can be controlled to be either anatase or TiO_2-B, depending on the reaction temperature. This may open up the way for further examinations of this ambient reaction in the presence of other alkali as well as alkaline earth hydroxides. Investigation of the catalytic and optoelectronic properties of these nanowires would also be interesting.

Acknowledgment. Financial support for this study was provided by the Hong Kong Polytechnic University.

Supporting Information Available: Raman spectra of the reaction products formed at 110 °C and TiO_2 anatase starting material (Figure S1), experimental refined atomic parameters using powder neutron diffraction of TiO_2-B (Table S1), low-magnification TEM micrograph of the 24-h product formed at 60 °C (Figure S2), and tabulated interplanar spacings derived from TiO_2-B (Table S2). This material is available free of charge via the Internet at http://pubs.acs.org.

References and Notes

(1) (a) Patzke, G.; Krumeich, F.; Nesper, R. *Angew. Chem., Int. Ed.* **2002**, *41*, 2446. (b) Rao, C. N. R.; Nath, M. *Dalton Trans.* **2003**, 1.

(2) (a) Hagfeldt, A.; Grätzel, M. *Chem. Rev.* **1995**, *95*, 49. (b) Matsuda, S. *Appl. Catal.* **1983**, *8*, 149. (c) O'Regan, B.; Grätzel, M. *Nature (London)* **1991**, *353*, 737. (d) Wang, P.; Zakeeruddin, S. M.; Moser, J. E.; Nazeeruddin, M. K.; Sekiguchi, T. Grätzel, M. *Nat. Mater.* **2003**, *2*, 402. (e) Tian, Z.-R.; Tong, W.; Wang, J.-Y.; Duan, N.-G.; Krishnan, V. V.; Suib, S. L. *Science* **1997**, *276*, 926. (f) Gouma, P. I.; Mills, M. J.; Sandhage, K. H. *J. Am. Ceram. Soc.* **2000**, *83*, 1007. (g) Bach, U.; Corr, D.; Lupo, D.; Pichot, F.; Ryan, M. *Adv. Mater.* **2002**, *14*, 845. (h) Bonhote, P.; Gogniat, E.; Campus, F.; Walder, L.; Grätzel, M. *Displays* **1999**, *20*, 137. (i) Zhou, Y. K.; Cao, L.; Zhang, F. B.; He, B. L.; Li, H. L. *J. Electrochem. Soc.* **2003**, *150*, A1246. (j) Zukalová, M.; Kalbáč, M.; Kavan, L.; Exnar, I.; Grätzel, M. *Chem. Mater.* **2005**, *17*, 1248.

(3) Hoyer, P. *Adv. Mater.* **1996**, *8*, 857.

(4) (a) Kasuga, T.; Hiramatsu, M. Hoson, A. *Langmuir* **1998**, *14*, 3160. (b) Kasuga, T.; Hiramatsu, M.; Hoson, A.; Sekino, T.; Niihara, K. *Adv. Mater.* **1999**, *11*, 1307.

(5) Du, G. H.; Chen, Q.; Che, R. C.; Yuan, Z. Y.; Peng, L. M. *Appl. Phys. Lett.* **2001**, *22*, 3702.

(6) Sun, X.; Li, Y. *Chem.—Eur. J.* **2003**, *9*, 2229.

(7) (a) Yao, B. D.; Chan, Y. F.; Zhang, X. Y.; Zhang, W. F.; Yang, Z. Y.; Wang, N. *Appl. Phys. Lett.* **2003**, *82*, 281. (b) Zhang, Y. X.; Li, G. H.; Jin, Y. X.; Zhang, J.; Zhang, L. D. *Chem. Phys. Lett.* **2002**, *365*, 300. (c) Seo, D. S.; Lee, J. K.; Kim, H. J. *J. Cryst. Growth* **2001**, *229*, 428. (d) Wang, W.; Varghese, O. K.; Paulose, M.; Grimes, C. A.; Wang, Q.; Dickey, E. C. *J. Mater. Res.* **2004**, *19*, 417.

(8) Nakahira, A.; Kato, W.; Tamai, M.; Isshiki, T.; Nishio, K.; Aritani, H. *J. Mater. Sci.* **2004**, *39*, 4239.

(9) (a) Ma, R.; Bando, Y.; Sasaki, T. *Chem. Phys. Lett.* **2003**, *380*, 577. (b) Ma, R. Z.; Fukuda, K.; Sasaki, T.; Osada, M.; Bando, Y. *J. Phys. Chem. B* **2005**, *109*, 6210.

(10) Chen, Q.; Zhou, W.; Du, G.; Peng, L. M. *Adv. Mater.* **2002**, *14*, 1208.

(11) Kukovecz, A.; Hodos, M.; Horvath, E.; Radnoczi, G.; Konya, Z.; Kiricsi, I. *J. Phys. Chem. B* **2005**, *109*, 17781.

(12) Du, G. H.; Chen, Q.; Han, P. D.; Yu, Y.; Peng, L. M. *Phys. Rev. B* **2003**, *67*, 035323.

(13) Yuan, Z. Y.; Su. B. L. *Colloids Surf. A* **2004**, *241*, 173.

(14) Daoud, W. A.; Xin, J. H. *Chem. Commun.* **2005**, 2110.

(15) Yoshida, R.; Suzuki, Y.; Yoshikawa, S. *J. Solid State Chem.* **2005**, *178*, 2179.

(16) (a) Armstrong, A. R.; Armstrong, G.; Canales, J.; Bruce, P. G. *Angew. Chem., Int. Ed.* **2004**, *43*, 2286. (b) Armstrong, A. R.; Armstrong, G.; Canales, García, R.; Bruce, P. G. *Adv. Mater.* **2005**, *17*, 862.

(17) Gao, X. P.; Lan, Y.; Zhu, H. Y.; Liu, J. W.; Ge, Y. P.; Wu, F.; Song, D. Y. *Electrochem. Solid State Lett.* **2005**, *8*, A26.

(18) Cromer, D. T.; Herrington K. *J. Am. Ceram. Soc.* **1955**, *77*, 4708.

(19) Baur, W. H. *Acta Crystallogr.* **1961**, *14*, 214.

(20) Marchand, R.; Brohan L.; Tournoux, M. *Mater. Res. Bull.* **1980**, *15*, 1129.

(21) Simons, P. Y.; Dachille, F. *Acta Crystallogr.* **1967**, *23*, 334.

(22) Latroche, M.; Brohan, L.; Marchand, R.; Tournoux, M. *J. Solid State Chem.* **1989**, *81*, 78.

(23) Banfield, J. F.; Veblen, D. R.; Smith, D. J. *Am. Mineral.* **1991**, *76*, 343.

(24) Banfield, J. F.; Veblen, D. R. *Am. Mineral.* **1992**, *77*, 545.

(25) Marchand, R.; Brohan, L.; Tournoux, M. *Mater. Res. Bull.* **1980**, *15*, 1129.

(26) Graymonprez, G.; Fiermanst, L.; Vennik, J. *Acta Crystallogr.* **1997**, *A33*, 834.

(27) Feist, T. P.; Davies, P. K. *J. Solid State Chem.* **1992**, *101*, 275.

(28) Catlow, C. R. A.; Cormack, A.; Theobalid, F. *Acta Crystallogr.* **1984**, *B40*, 195.

(29) Brohan, L.; Verbaere, A.; Tournous, M.; Demazeau, G. *Mater. Res. Bull.* **1982**, *17*, 335.

(30) Tournoux, M.; Marchand, R.; Brohan, L. *Prog. Solid State Chem.* **1986**, *17*, 33.

(31) Zukalová, M.; Kalbáč, M.; Kavan, L.; Exnar, I.; Heeger, A.; Grätzel, M. *Prog. Solid State Chem.* **2005**, *33*, 251.